Discrete element modelling of granular materials

S. van Baars
Delft University of Technology, Faculty of Civil Engineering, Geotechnics

A new model is developed by the author, which does not use the equations of motion but the equations of equilibrium to describe granular materials. The numerical results show great similarities with reality and can generally be described by an advanced Mohr-Coulomb model. However, many contacts between the grains will collapse not due to shear deformation as Coulomb suggests, but due to tension failure. These micro cracks occur always in the direction of the major principal stress, which might be a different direction than the observed failure surface.

Keywords: **Discrete elements, shear bands, crack growth**

Introduction

De Josselin de Jong and Verruijt (1969) have developed a method to determine the magnitude and the direction of the contact forces between grains, by measuring the rotation of polarised light through these grains made of photoelastic materials. In this way the local displacements and forces could be studied. About ten years later Cundall developed a computer model, named Ball, to describe the behaviour of granular materials. This model is based on the basic elements of these materials, i.e. the grains themselves and their interactions. The method is validated by Cundall and Strack (1979) by comparing force vector plots obtained from the computer program Ball with the corresponding plots obtained from the photoelastic analysis, which was done by De Josselin de Jong and Verruijt. One of the major problems with the model of Cundall was the computational time. According to Ting (1989) it is not feasible to simulate more than a few tens of thousands of grains, even with the fastest super computers currently available.
Lindhout (1992) has tried to model the cylinder test with Trubal, which is the successor of Ball. Due to compaction problems, stability problems and the large computation time this could not be done. Therefore a new research project has been set up to solve these problems. The idea was that if the quasi-dynamic analysis of Cundall, which is using artificial damping, can be replaced by a technique which is using the so called finite element method, the model will become more useful. In the following section the modelling of granular materials with discrete elements will be discussed. With the new model based on the equations of equilibrium firstly the behaviour of non-cohesive materials and secondly the behaviour of cohesive materials are discussed.

Discrete element modelling

Discrete element modelling, which is also called distinct element modelling, is in fact a type of finite element modelling, in which every element represents one grain. The main difference is that due to deformation some contacts between the grains can break and new contacts can be made. Because of this the global stiffness matrix of the complete structure has to be rebuild constantly. For non-cohesive materials there is also a second reason why this matrix has to be updated; the behaviour of the contacts, both in normal as in shear direction is not linear, which means that the stiffnesses k_n and k_s of these contacts have to be recalculated continuously.
If the boundary conditions of the structure (forces or displacements) are changed, then this will effect every grain. All grains will displace in such a way that a new force equilibrium has been created (quasi-static approach) or a new time step has been reached (dynamic approach).
Until recently only the dynamic approach has been worked out, mainly by Cundall. His model is based on the equations of motion. For this research the quasi-static approach will be used, which is based on the equations of equilibrium. Both models will be worked out for a two-dimensional rectangular Cartesian (OXY)-field.

Micro modelling
The behaviour of granular structures depends on the individual grains and their interaction.
In order to be able to model this on a microscopic level, three simplifications are made.
The first is made due to the number of dimensions. Three-dimensional computer modelling consumes a lot of time and memory. Because of its simplicity, two-dimensional modelling gives more insight in the obtained results.
The second simplification is made to the grain shape. The most common one, a circle, reduces the calculation substantially. However, circular grains will roll easier than grains with a more complex shape. Like this, elliptical grains show a later failure than circular grains during a loading test according to Rothenburg and Bathurst (1992).
The description of the contact behaviour between two grains contains the last simplification. This behaviour is divided in three parts:

1. Normal deformation.
2. Shear deformation.
3. Slip or crack.

All differences between real measurements and model results have to be explained by these three simplifications.
The relation between the normal force F_n and the normal displacement n is given by:

$$F_n = k_n n \tag{1}$$

For cohesive materials this stiffness in normal direction k_n is constant, but for non-cohesive materials this is not constant because it depends on the normal displacement.

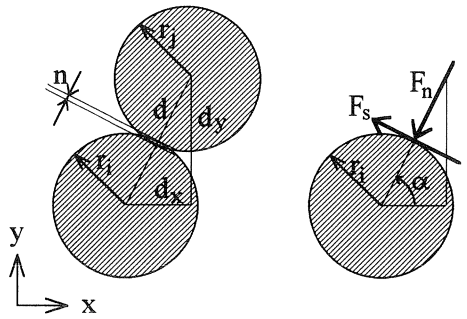

Fig. 1. Definition of micro parameters.

The force-displacement relation of two balls in normal direction is solved by Hertz (1881). (The definitions of the micro parameters are presented in Fig. 1.)

$$k_n = M\sqrt{n} \tag{2}$$

in which:

$$M = \frac{2\sqrt{2\tilde{r}}G_\mu}{3(1-v_\mu)} \quad \text{and} \quad n = r_i + r_j - d \quad \text{and} \quad \tilde{r} = \frac{2r_i r_j}{r_i + r_j}$$

The grain stiffness M depends on the shear modulus G_μ and the Poisson's ratio v_μ of the material of the grain, but also on the average size $\tilde{r}$ of both grains. The reason why this relation is not linear for non-cohesive granular materials is that the contact surface between the grains depends on the deformation, so during loading the geometry is not constant. This causes a non-linear stress-strain behaviour.
The force-displacement relation in shear direction between two balls is solved by Mindlin and Deresiewicz (1953) and verified by Deresiewicz (1958). The shear force F_s is proportional to the shear displacement s_h for the elastic area.

$$F_s = k_s s_h \tag{3}$$

The stiffness in shear direction k_s can be related to the stiffness in normal direction:

$$k_s = \kappa_v k_n \tag{4}$$

in which:

$$\kappa_v = 3\frac{1-v_\mu}{2-v_\mu}$$

This means that the relation between the stiffnesses of the normal and shear direction depends only on the Poisson's ratio v_μ of the grain material.

Motion modelling

The modelling of granular structures can be divided in four phases:

1. Creation of the particles.
2. Calculation of the boundary conditions like wall displacements.
3. Calculation of the grains.
4. Calculation of wall forces and other desirable information.

In the model of Cundall, based on the equations of motion, all grains will be, for every time step, one by one checked and recalculated in this phase 3.

This calculation of the grains consists of three parts:

A. With the two force-displacement relations, $F_n = k_n n$ and $F_s = k_s s_h$ all forces on one particular grain are calculated.

B. With these forces and the equations of motion (second law of Newton), the acceleration of the grain is determined:

$$\sum \vec{F} = m\ddot{\vec{x}} \tag{5}$$

in which:

m = mass of a grain

$\ddot{\vec{x}}$ = acceleration of a grain or second derivative of its place

For the next time step, the new position of the grain is found with two integration steps:

$$\vec{x} = \frac{1}{m}\int\int\left(\sum \vec{F}\right)dt\ dt \tag{6}$$

This integration is not very stable and therefore small time steps and damping are necessary. Extra calculation time and less accuracy are the result of this.

C. All contacts of the grain are checked for:

I. Plastic deformation (slip or crack).

if $|F_s| > f_{gg}F_n + F_t$ then $|F_s| = f_{gg}F_n$ (7)

in which:

$f_{gg} = \tan\phi_\mu$ and $F_t = c_\mu \bar{r}^2$ or $F_t = c_\mu r_i r_j$

II. Contact breaking.

if $-F_n > F_t$ then *break contact* (8)

III. Contact making.

if $n > 0$ then *make contact* (9)

With the new positions the new forces for part A. can be calculated. In this way, for every time step, all contact forces and grain positions are determined. The computer models Ball, Trubal and PFC (particle flow code) of Itasca Minneapolis are based on this method.

Equilibrium modelling

The new model is based on the equations of equilibrium. Only part B in which the displacements of the grains are calculated is different from the motion modelling:

A. The first part is equal to the motion model.

B. In the new approach, equilibrium equations are used instead of equations of motion:

$$\sum F_x = 0 \qquad \sum F_y = 0 \qquad \sum M = 0 \tag{10}$$

By disregarding time, dynamic problems like explosions, vibrations and quakes can not be modelled. The three equations form a 3×3 matrix:

$$\begin{bmatrix} \sum_{k=1}^{n_{c/g}} -c^2k_n - s^2k_s & \sum_{k=1}^{n_{c/g}} (k_s - k_n)sc & \sum_{k=1}^{n_{c/g}} srk_s \\ \sum_{k=1}^{n_{c/g}} (k_s - k_n)sc & \sum_{k=1}^{n_{c/g}} -s^2k_n - c^2k_s & \sum_{k=1}^{n_{c/g}} -crk_s \\ \sum_{k=1}^{n_{c/g}} srk_s & \sum_{k=1}^{n_{c/g}} -crk_s & \sum_{k=1}^{n_{c/g}} -r^2k_s \end{bmatrix} \begin{bmatrix} \Delta x \\ \Delta y \\ \Delta\phi \end{bmatrix} \begin{bmatrix} \sum_{k=1}^{n_{c/g}} cF_n + sF_s \\ \sum_{k=1}^{n_{c/g}} sF_n + cF_s \\ \sum_{k=1}^{n_{c/g}} -rF_s \end{bmatrix} \tag{11}$$

in which:

$n_{c/g}$ = number of contacts per grain.

s = $\sin(\alpha)$

c = $\cos(\alpha)$

r = radius of the grain

All forces and stiffnesses on one particular grain are placed in this matrix. The displacements of the grains can directly be calculated with Gauss elimination.

C. The third part is equal to the motion model.

Although the equilibrium position is directly calculated, the displacement of a grain will effect its neighbouring grains. Therefore several iterations through the whole structure are necessary to find the total equilibrium state of the grain structure. The computer model Grain, written by the author, is based on this method.

Because the grains can gain and loose contacts during the simulation not only the calculation of the grains but also the book-keeping of the grain and contact data is important. It is time consuming to check every time all possible grain contacts. To avoid this, each grain has a list of the contacts between its neighbours and also a list of the grains which are nearby but not connected. These are called friends. After the grains are sprinkled between several walls, the entire group of grains is considered as a village surrounded by city walls. Every grain has to check the complete village in order to make its personal list of friends. This has to be done only once after the creation of the grains and every time a grain has been displaced outside his defined friend-area. This happens only occasionally. In this way only the friends have to be checked for contact-making and the neighbours for contact-breaking.

Motion versus equilibrium

The main advantage of the motion model is that it can handle dynamic problems, although this is most of the times not necessary. The main advantage of the equilibrium model is the speed.
When this research was started in 1993, one of the most used motion models was New Trubal (NTB) from Cundall. The final results for both models were found to be equal, although GRAIN was much faster. For each iteration step of GRAIN, 4000 iteration steps were necessary with NTB. Because NTB was not able to handle certain characteristic tests and needed to much calculation time, only GRAIN is used to do the rest of the numerical simulations in this paper.
Two years later (February 1995) a new version called Particle Flow Code (PFC) was released by Itasca. It had two major improvements:

1. PFC could, although in a complicated way, use stress controlled walls.
2. The calculation speed had increased a lot.

Although the models are based on various basic principles, the final results are quite similar. The only difference is now that PFC (motion) uses fifty times more iteration steps than GRAIN (equilibrium).

Non-cohesive granular materials

A discrete element model is a perfect tool for measuring the influence of a number of specific micro parameters (like the relative density, lateral pressure or the internal friction) on the macro behaviour of non-cohesive granular materials.
Especially, fundamental issues like the failure mechanism can be analysed.

Failure mechanism

In Fig. 2 a sample is failing during a biaxial test. The question is if this happens because of the slipping of the grains or the rolling of the grains or maybe a combination of both. Therefore the number of contacts per volume of this sample is measured. During loading the number of axial (vertical) contacts increases a little bit, but the number of lateral (horizontal) contacts decreases strongly. This can be seen in Fig. 3. This decrease of horizontal contacts is a sign of the failure mechanism of granular materials. In horizontal direction so many contacts are lost that the grains can roll away.

This failure behaviour becomes clearer if we look at the influence of the internal friction.
This internal friction between the grains f_{gg}^{ll} is one of the most important micro parameters. In Fig. 4 two macro parameters are strongly influenced by an increase of the internal friction, namely the strength of the whole structure is increasing, and the dilatancy is increasing as well.

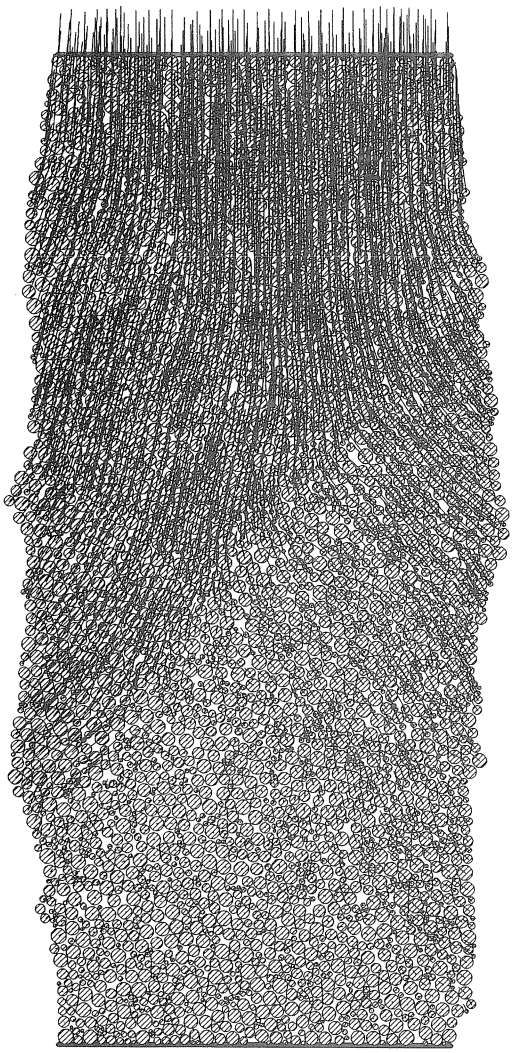

Fig. 2. Biaxial test: displacements of 4000 non-cohesive grains,

When the internal friction f_{gg}^{II} is zero, the grain structure will shear under any circumstance to the maximum relative density. In this way the structure will behave like a fluid. The volume will remain constant. This behaviour is very clear in the numerical simulation.
On the contrary, a structure with infinite friction can collapse only by the rolling of the grains. Triangle contact groups do not role, but quadrangular and more angular contact groups are able to deform despite the infinite friction.

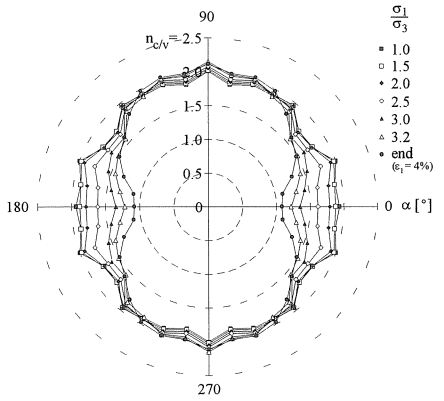

Fig. 3. Number of contacts per volume versus the contact angle during a biaxial test.

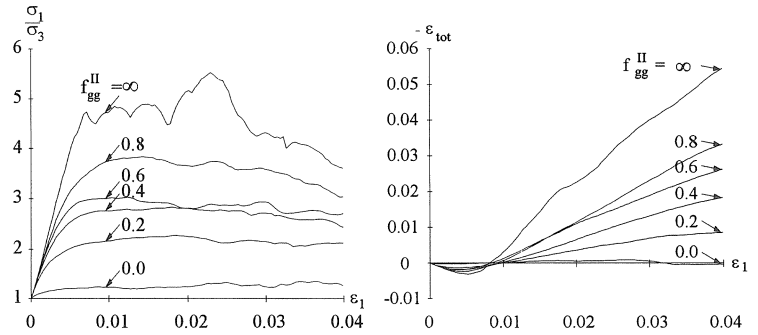

Fig. 4. Biaxial test: influence of the internal friction.

These rolling groups will act like rolling wedges, causing an increase of the pore volume and a decrease of the number of contacts in the shear bands. This dilatancy will be largest for infinite friction, because all wedges will be mobilised, and not one will fail because of shearing.

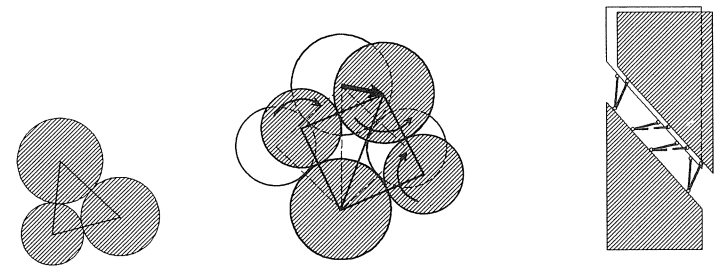

No rolling *Rolling without shear* *Dilatancy and contact breaking*

Fig. 5. Failure on micro scale.

Also another conclusion can be drawn from these results. Even if the friction is infinite, the strength will not be infinite. This means that for structures with a low friction the strength is mainly determined by the friction, but for a high friction the strength is mainly defined by the rolling of the grains.
Other tests show that if the rotation of the grains is fixed in combination with an infinite friction, then an infinite strength is found, which is in agreement with the previous theory. So, the rotation of the grains is very important in the discrete element modelling.
It can be concluded that non-cohesive granular materials fail because of both shearing and rolling. Only the rolling of the grains is causing dilatancy and contact breaking.

Continuum behaviour of non-cohesive materials

Generally all tests with GRAIN can be described with an advanced Mohr-Coulomb model. The stiffness behaviour of non-cohesive materials has been solved by Van Baars (1995 and 1996).
The Young's modulus is not constant but depends on the stress.

$$E_{50} = E_{ref}\left(\frac{\sigma_0}{\sigma_{ref}}\right)^{\beta} \tag{12}$$

in which:.

$$E_{ref} = \left(\frac{\sqrt{\sigma_{ref}}G_{\mu}}{3(1-\upsilon_{\mu})}n_{c/v}\right)^{\frac{2}{3}} \frac{2\kappa_v}{\kappa_v + 1}$$

$$\beta = \frac{1}{3}$$

$$\sigma_0 = \frac{(\sigma_1 + \sigma_2)}{2}$$

$$\kappa_v = 3\frac{1-\upsilon_{\mu}}{2-\upsilon_{\mu}}$$

$$n_{c/v} = \frac{n_c}{n_v} = \frac{\bar{d}^3 n_c}{V}$$

This theoretical solution is in good agreement with the numerical results of the Young's modulus found by Grain.

Shear band development

Very interesting is the direction of the shear band. Fig. 6 shows the grain displacements of two different biaxial tests from 5% to 10% deformation. The sample on the right had no wall friction, so the weakest areas were near the top and the bottom. Only there the grains bend away at failure.
The sample on the left has its weakest point in the middle because of the reinforcement at the walls

caused by the shear stresses. A clear shear band is formed in the centre with a direction of $\theta = 52° \pm 2°$. This is the same as suggested by the advanced Mohr-Coulomb theory, namely

$$\theta = 45° + \frac{\psi}{2} = 45° + \frac{14.2°}{2} \approx 52° \tag{13}$$

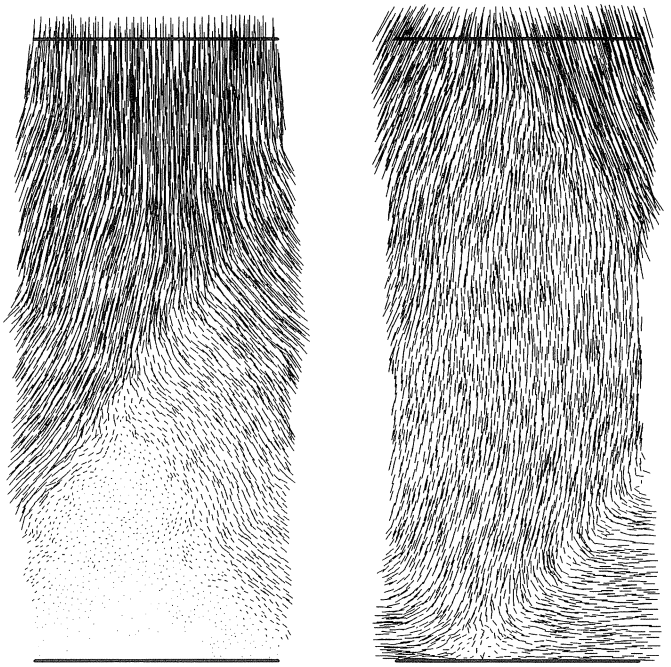

With wall friction *Without wall friction*

Fig. 6. Biaxial test: displacements of the grains.

Simple shear test

The failure mechanism in the simple shear test of Roscoe (1970) is still surrounded by questions. Therefore this test is also modelled. Three different failure mechanisms have beeen suggested:

- Horizontal shearing in the analogy to the shear law of Coulomb.
- Vertical shearing according to De Josselin de Jong (1992).
- Lateral failure according to the author.

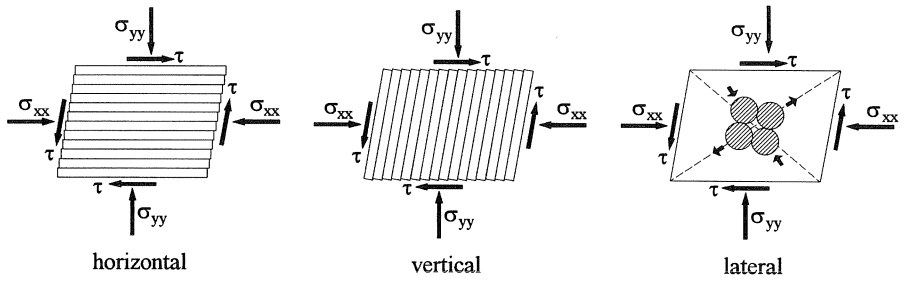

Fig. 7. Failure mechanisms.

If failure occurs by exceeding of the maximum shear stress in a certain direction, which is suggested by the Coulomb criterion, then only the stress and deformation fields of the horizontal and vertical failure mechanisms are both static and kinematic admitted. In that case, for the horizontal mechanism the horizontal stress during failure has to be:

$$\sigma_{xx} = \frac{1 + \sin^2(\phi')}{1 - \sin^2(\phi')}\sigma_{yy} \tag{14}$$

and for the vertical mechanism:

$$\sigma_{xx} = \frac{1 - \sin^2(\phi')}{1 + \sin^2(\phi')}\sigma_{yy} \tag{15}$$

When the horizontal stress does not meet these particular values by any (artificial) way, no failure can occur according to the Coulomb criterion. This can not be the case.
If failure takes place by breaking of contacts in the direction of the minor principal stress, because tension forces can not be absorbed on micro level, then only lateral failure can occur. This means also that the shear direction can not be obtained from the Coulomb line. This statement can easily be verified with GRAIN by comparing the average rotation of the grains γ_μ with the rotation of the vertical walls γ. The ratio of these rotations during failure is for the horizontal, vertical and lateral mechanism respectively equal to:

$$\frac{\gamma_\mu}{\gamma} = 0.0 \text{ or } 1.0 \quad \text{or} \quad 0.5 \text{ respectively} \tag{14}$$

The dashed line of Fig. 8 shows that the diagonal failure mechanism is the only correct one $\left(\frac{\gamma_\mu}{\gamma} \approx 0.5\right)$. During failure up to 25% of the contacts are broken, which correspond with this mechanism as well.
The results of the simple shear tests with infinite wall friction presented in Fig. 8 can be predicted quite accurately by the results of biaxial tests using the advanced Mohr-Coulomb model, although the shear modulus is a little bit too small.

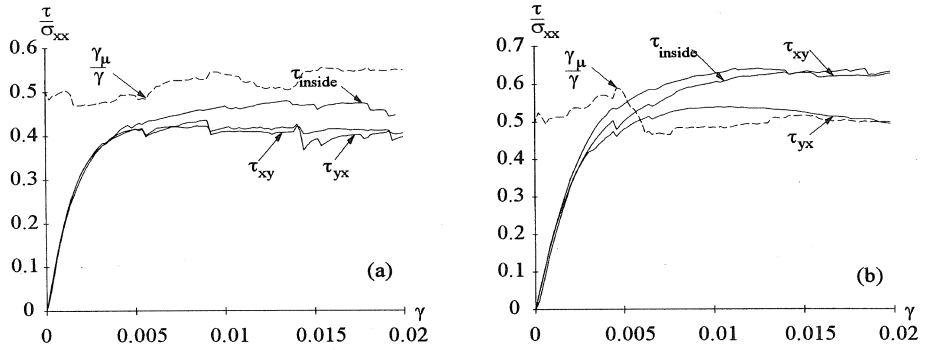

Fig. 8. Simple shear: Test I: $\sigma_{xx} = \sigma_{yy} = 1$ bar (a) and Test II: $\sigma_{xx} = 1$ bar, $\sigma_{yy} = 2$ bar (b).

According to the advanced Mohr-Coulomb theory, the major principal direction β during a test should be similar for the (inside) stresses and strains. This behaviour is also found for GRAIN for both simple shear tests and is presented in the Fig. 9. The theoretical major principal direction during failure is solved by:

$$\cos(2\beta) = -\frac{1}{\sin(\phi)}\frac{(\sigma_{yy} - \sigma_{xx})}{(\sigma_{uu} - \sigma_{xx})} \tag{16}$$

So:

$\beta = 45°$ for simple shear I

$\beta = 64°$ for simple shear II

This so called coaxiality suggest that the rolling of the grains during failure will be on average in the direction of the minor principal stress. In other words, the grains escape in the direction of the lowest resistance.

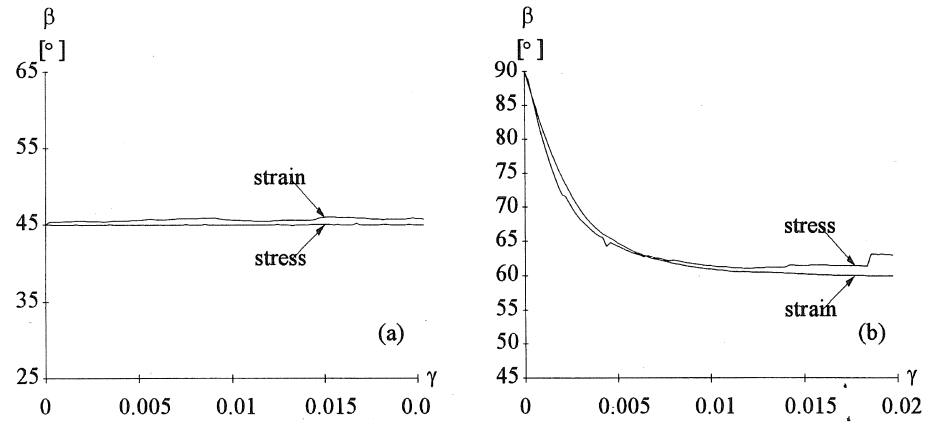

Fig. 9. Principal directions of stress and strain: Test I (a) and Test II (b).

Cohesive granular materials

Default parameters

In order to gain some insight in the failure mechanism and the moment of failure of cohesive granular materials, several biaxial tests are modelled in Grain. The default micro parameters are chosen to be representative for sandstone with a dense compaction.

The linear spring constant is $k_n = 1$ MN/m. To obtain a sample with a high density this friction between two grains will be temporarily decreased to zero $f_{gg}^{I} = 0.0$ before cementation. The wall friction is for all tests zero $f_{gw} = 0$. The cohesion c'_{μ} is unknown and is chosen to be 100 MPa in order to give the sample more or less the same strength as Castlegate sandstone (USA).

The average grain size is $\bar{r} = 0.1$ mm. The default confining pressure is chosen to be $\sigma_3 = 10$ bar = 1 MPa. The total deformation of 2% is reached in half an hour on a normal personal computer with 500 load steps: $\frac{\Delta H}{H} = 4.0 \times 10^{-5}$. Twenty iterations per loading step were sufficient to iterate accurately enough to the equilibrium state. The depth of the sample is chosen to be equal to the average diameter of the grain ($D = \bar{d} = 2\bar{r}$) to be able to calculate the stresses.

Continuum modelling

Fig. 10 presents the rotations of the grains in a sample of 4000 grains at failure. Before the test all radial lines on the grains were pointing upwards. These lines indicate that only the broken grains within the shear band are rolling.

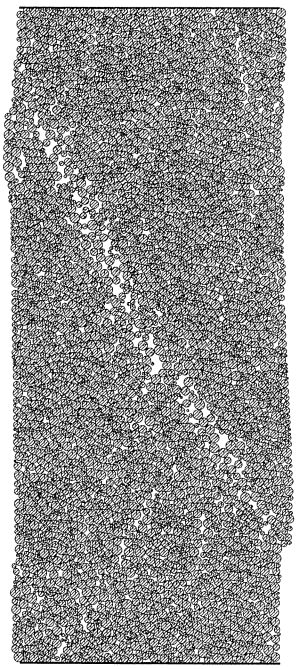

Fig. 10. Failure surface during a biaxial test on 4000 grains.

Several biaxial tests like this are done on samples with identical micro parameters but with different shapes of the sample and different grain size distributions. According to Fig. 11 the stiffness and the strength of the samples were all found to be quite similar. The percentage of the broken contacts is reflected by the dashed line in the same figure.

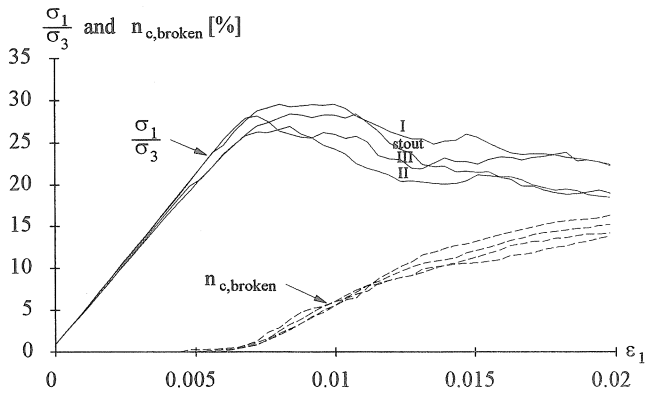

Fig. 11. Biaxial test: different shapes.

Compression tests, confined biaxial tests and unconfined biaxial tests all give comparable results for the Young's modules and the Poisson's ratio. These parameters are listed in the Table 1. At the beginning of a test the measured values are a little bit lower than just before failure, because during the compression of a sample extra (non cohesive) contacts are formed. These contacts increase the total stiffness of the sample.

Table 1. Young's modules and Poisson's ratio.

Test	E (GPa)	v
Compression	3.9–4.2	0.11–0.13
Confined Biaxial	3.8–4.2	0.04–0.19
Unconfined Biaxial	3.9–4.2	-

Van Baars (1995) shows analytically that both the stiffness behaviour and the strength behaviour of cohesive granular materials can be described by the Mohr-Coulomb model. The Young's modulus of cohesive granular materials depends only on the Poisson's ratio, the number of contacts per volume, the normal spring constant and the average grain size:

$$\frac{E}{1-v} = n_{c/v}\frac{k_n}{2\bar{d}} \qquad \text{in which} \qquad n_{c/v} = \frac{\bar{d}^3 n_c}{V} = 1.80 \tag{17}$$

So,

$$E = (1-0.1)\times 1.80\times \frac{10^6}{2\times 2\times 2210^{-4}} = 4.05 \text{ GPa} \tag{18}$$

Which is a nice analytical prediction.

Very interesting is the fact that the strength of a sample is hardly influenced by the grain size distribution. Distribution A contains more small grains than large grains, while the distribution B is linear. For both grain size distributions the moment of failure of the samples can be accurately described by the Mohr-Coulomb parameters c' and ϕ' (Table 2). The different distributions cause only a very small difference in the strength of the samples. This means that although the formation of micro cracks depends on the average of the contact forces and the deviation of these forces, both the average force and its deviation do not depend on the distribution of the grain sizes.

Table 2. Cohesion and angle of internal friction.

Type	c'	ϕ'
A	9.3 MPa	22°
B	9.6 MPa	22°

Van Baars (1995) shows analytically that this is true. The angle of internal friction is constant and does not depend on the contact force distribution. The cohesion depends only on the average strength of a single (lateral) contact and on the number of contacts per micro volume:

$$\sin\phi' = \frac{1}{3}$$

$$c' = \frac{c_{\mu} n_{c/v}}{16\sqrt{2}} \qquad \text{with} \qquad n_{c/v} = \frac{\bar{d}^3 n_c}{V} \tag{19}$$

So, in this case:

$$\phi' = 19.5°$$

$$c' = \frac{100 \text{ MPa}\times 1.80}{16\sqrt{2}} = 8.0 \text{ MPa} \tag{19}$$

The deviation with the numerical angle of internal friction and cohesion of Table 2 is not too large.

Contact forces and failure mechanism

The strength and the elasticity of the granular structure could not be solved without the analytical solution for the average normal and shear forces related to biaxial tests:

$$\bar{F}^{II}_{n,\alpha} = \bar{F}^{I}_{n}\left(c^2 + \frac{\sigma_1}{\sigma_3}s^2\right)$$

$$\bar{F}^{II}_{s,\alpha} = \bar{F}^{I}_{n}\left(1 - \frac{\sigma_1}{\sigma_3}\right)cs \qquad (20)$$

in which

$$\bar{F}^{I}_{n} = 2\frac{\sigma_3 V}{n_c \bar{d}} \qquad \text{or:} \qquad \bar{F}^{I}_{n} = 2\frac{\bar{d}^2\sigma_3}{n_{c/v}}$$

These average normal and shear forces (dashed lines in the next figures) in relation to the angle between the contact and the horizontal axis, are in good agreement with the average forces found by simulating a sandstone sample of 1000 grains at 10 MPa loading pressure with Grain.
The radar plot of these forces on the right shows that the measured normal forces are almost identical to the analytical solution. The average normal force will always be positive (pressure). Still it is found that failure occurs always due to local tension failure. This means that not only the average value of the normal force is important, but also the deviation of the forces.
The normal forces are, especially for the horizontal contacts, very small. During loading the deviation of the forces will increase, while the average normal force of the horizontal contacts remains constant. Thus, these contacts will collapse first due to tension failure. This means that mainly axial (vertical) micro cracks are expected, since the cracks are perpendicular to the broken contacts.

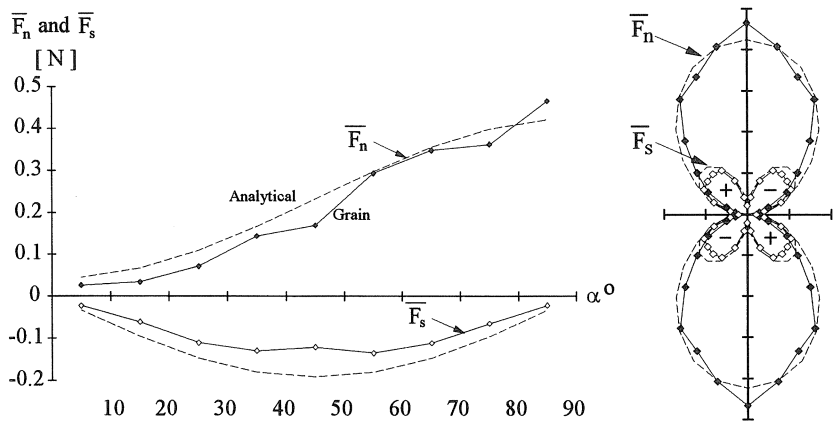

Fig. 12. Biaxial test: average normal and shear forces.

One of the most interesting phenomena of the failure of a sandstone sample is the nucleation and growth of a crack. Fig. 13 shows the failure mechanism of a cohesive granular material in detail. If cemented contacts are broken then a thick line perpendicular on the contact is drawn. The horizontal walls are also represented by thick lines, the rubber vertical membranes are not drawn.

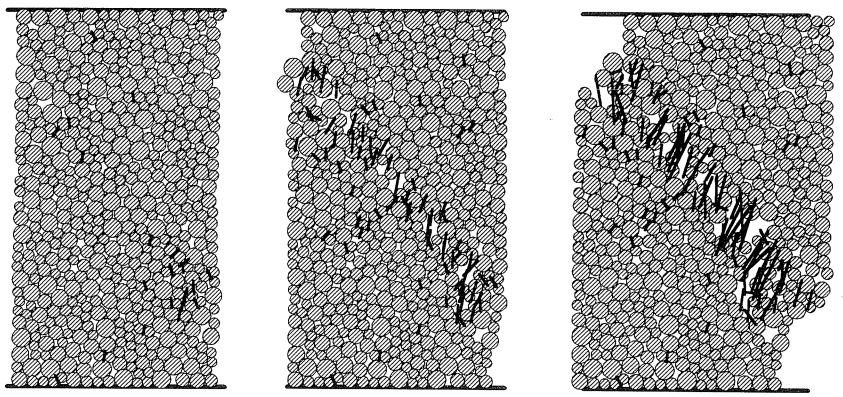

Phase A *Phase B* *Phase C*

Fig. 13. Failure mechanism of a cohesive granular material.

The failure mechanism of a cohesive granular material can be divided into three phases:

Phase A. During loading more and more contact forces become negative as predicted in the previous paragraph. They break because of local tension failure and not because of shear failure as Coulomb suggests.

Phase B. A crack weakens the surrounding area and increases the probability of a new crack in this area. In this way a failure surface is formed. Although this surface is diagonal, the micro cracks are mainly vertical, which means that mainly horizontal contacts are broken. This phenomenon is also found for concrete and mortar by Stroeven (1973). Failure was caused for these materials by axial tensile (cleavage) cracks.

Phase C. Grains with broken contacts act as rollers between the lower and upper part of the sample. The resistant vertical force becomes less and less.

Three point bend test

A familliar test to measure the strength of a concrete beam is the three point bend test. Therefore this test is also simulated with a small beam containing a thousand grains ($h \times l \times d$ = 39.8 cm × 102.5 cm × 2.00 cm). Before failure the beam on the left shows in Fig. 14 a very clear arch of compressive forces from the left support upwards to the vertical load and downwards to the right support. The underside of the beam has mainly horizontal tensile forces with small vertical compressive forces, which is in analogy with the forming of the small perpendicular tensile forces in the biaxial test. In other words, the results are as expected.

The crack in the beam on the right formed during failure, starts at the bottom of the beam and grows from weaker area to weaker area, which are the larger pores. A crack can also be dead ending

if the area above the crack is too strong. In that case another crack parallel to the former crack will appear and extend the total failure surface. The micro cracks are indeed in the direction of the major principal stress.

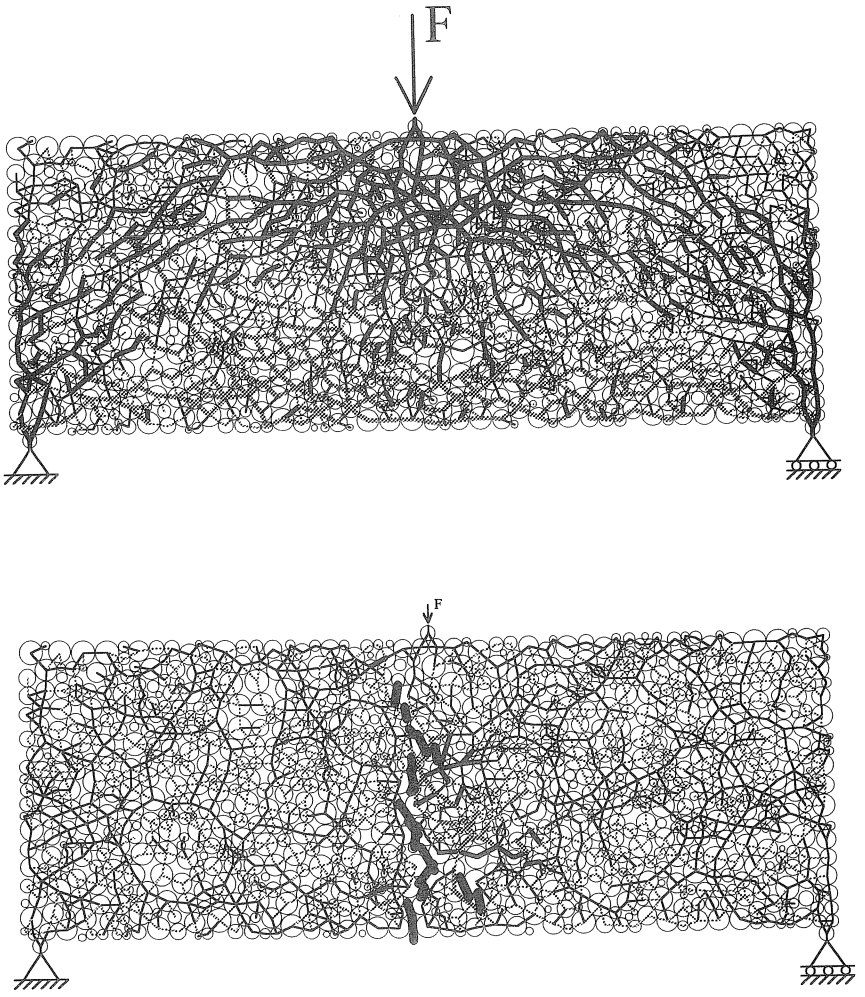

Fig. 14. Concrete beam before (a) and after (b) failure.

Conclusions

Models based on equilibrium will give the same results for quasi-static problems as models based on motion. Equilibrium models will iterate faster but can not be used for dynamical problems like the models based on motion. The results from the discrete element models show in a qualitative

way a good similarity with real tests on granular materials. These results can be described with an advanced Mohr-Coulomb model. The Coulomb line describes the moment of failure of a granular material quite well, although the present approach suggests that failure will not occur due to shear failure but due to tensile failure on a microscopic level, which is causing tension cracks in axial direction.

References

Baars, van S. (1995), Discrete element analysis of granular materials. Communications on Hydraulic and Geotechnical Engineering, Report No. 95-4. ISSN 0169-6548.

Baars, van S. (1996), Discrete element analysis of granular materials. Dissertation, Technische Universiteit Delft, ISBN 90-9009494-6.

Cundall, P.A. and Strack, O.D.L. (1979), A discrete numerical model for granular assemblies. Géotechnique, volume 29, pp. 47–65.

Deresiewicz, H. (1958), Reprinted from: Mechanics of granular matter. Advances in Applied Mechanics, volume 5, Academic press inc., New York, pp. 254–261.

Hertz, H. (1881). Journal of Mathematics, volume 92.
Or: Timoshenko, S. and Goodier, J.N. (1951): Theory of elasticity. McGraw-Hill Book Company, Inc. pp. 372–383.

Josselin de Jong, de G. and Verruijt A. (1969), Etude photo-élastique d'un empilement de disques. Cahiers du Group Français de Rhéologie, Janvier 1969, volume II, pp. 73–86.

Josselin de Jong, de G. (1992), Co-rotational solution in simple shear test. Proceedings of the Wroth memorial symposium, Predictive Soil Mechanics, Thomas Telford, London, pp. 254–260.

Lindhout, P.H. (1992), Use of distinct element method in soil and rock mechanics. student report 92.048, Shell, March 1992, pp. 39–41.

Mindlin, R.D. and Deresiewicz, H. (1953), Elastic spheres in contact under varying oblique forces. Journal of Applied Mechanics, volume 20, September 1953, pp. 327–344.

Roscoe, K.H. (1970), The influence of strains in soil mechanics. Géotechnique, volume 20, no. 2, pp. 132–141.

Rothenburg, L. and Bathurtst, R.J. (1992), Micromechanical features of granular assemblies with planar elliptical particles. Géotechnique, volume 42, no. 1, pp. 79–95.

Stroeven, P. (1973), Some aspects of the micromechanics of concrete. Dissertation, University of Technology Delft, February 21st 1973, pp. 156–165.

Ting, T.M. (1989), Discrete numerical model for soil mechanics. Journal of Geotechnical Engineering, volume 115, no. 3, March 1989, p. 381.